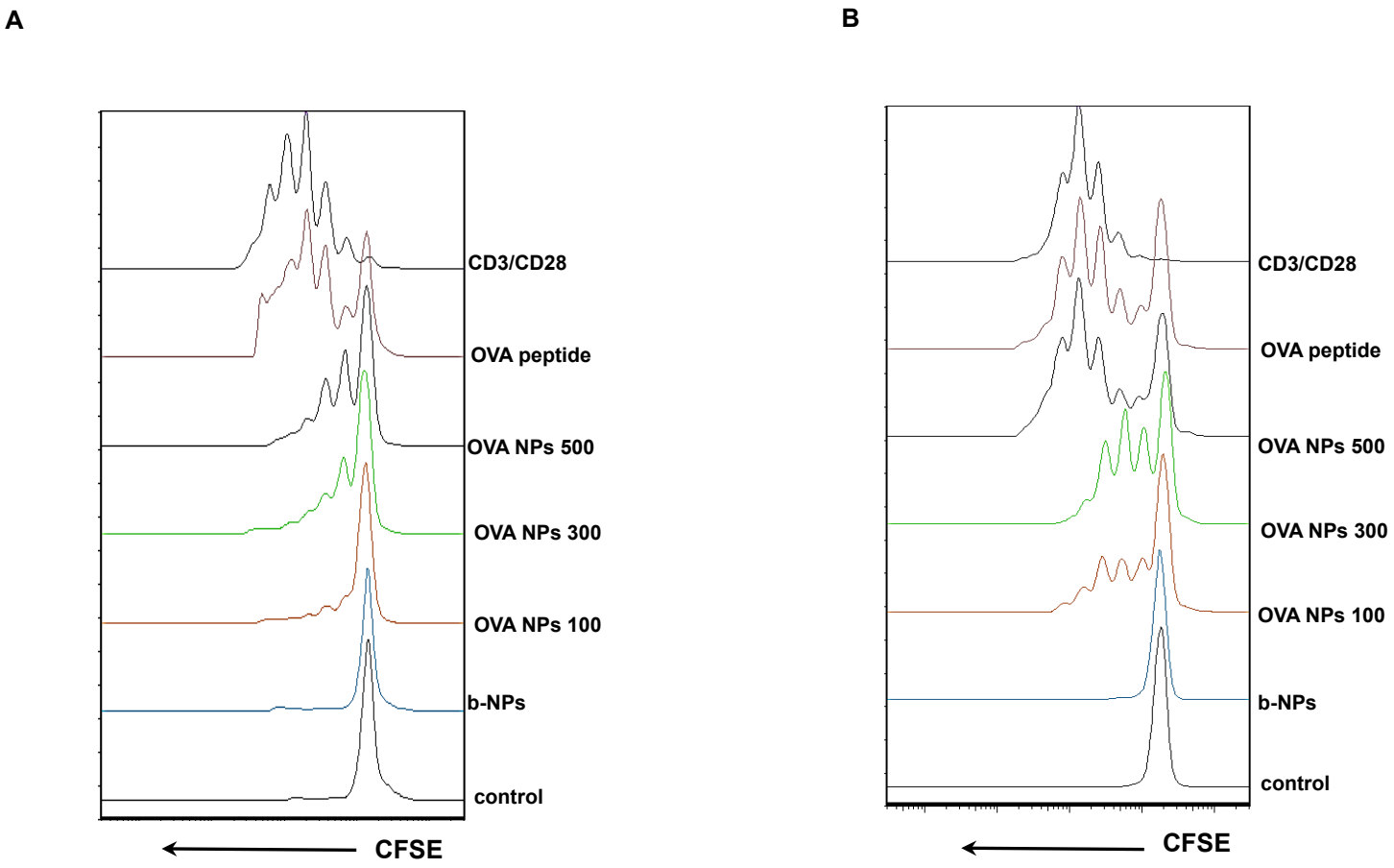

Supplementary Figure 1: OVA-nanoparticles activate BMDCs *in vitro* and consequently stimulate antigen specific T cells. Representative flow cytometric histogram demonstrating proliferation profiles of OT-II $CD4^+$ (**A**) and OT-I $CD8^+$ (**B**) CFSE labeled T cells following co-culture with BMDCs unpulsed and pulsed with b-NPs, various concentrations (μg/ml) of OVA-NPs, OVA peptide ($OVA^{323-339}$/$OVA^{257-264}$), or with anti-CD3 and anti-CD28 antibodies alone (control).

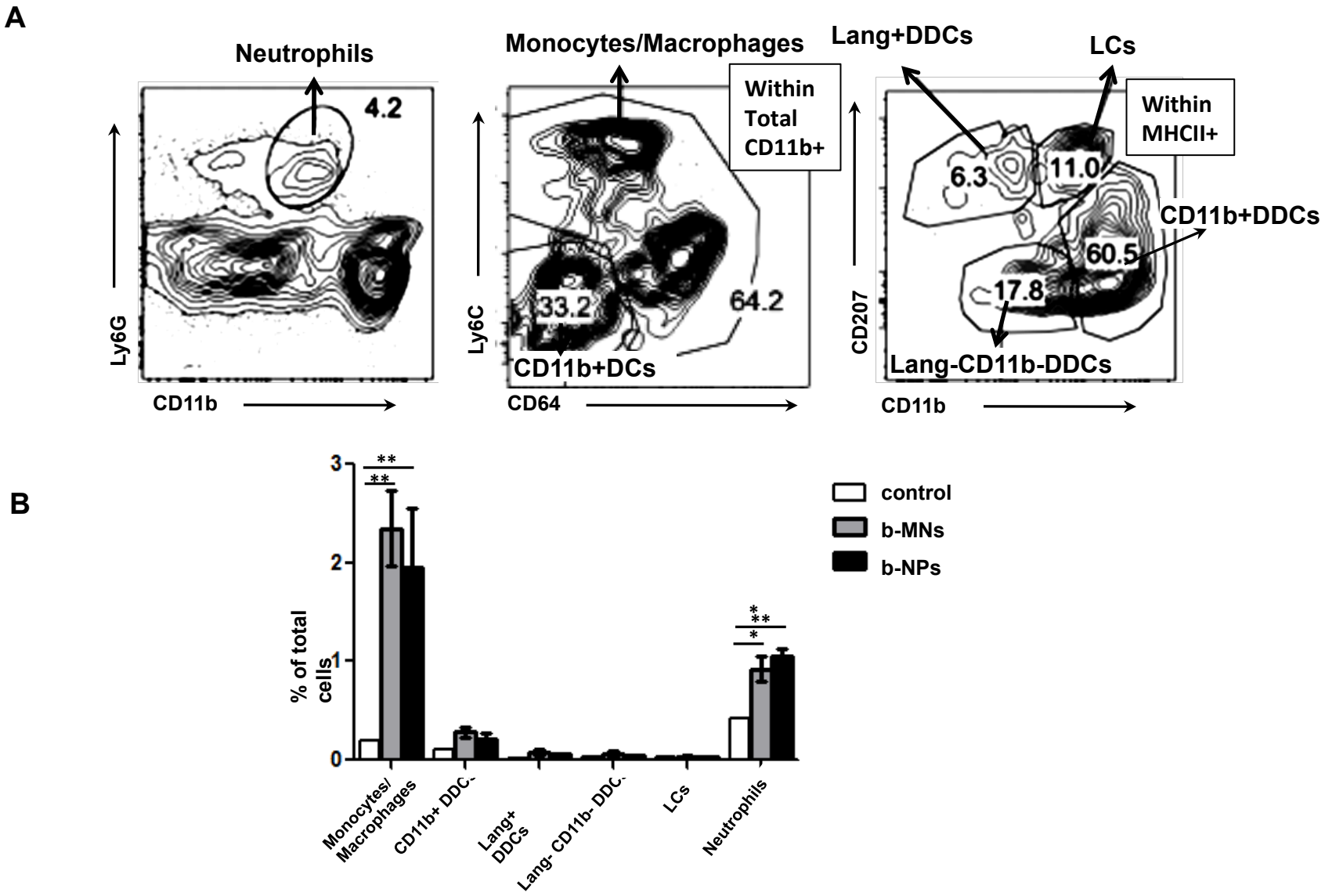

Supplementary Figure 2: Recruitment of innate immune cells 24 hours following microneedle intradermal application. A) FACS analysis demonstrating the gating strategy used for identification of different infiltrating cell types isolated from the ear skin. Neutrophils were gated as Ly6G$^+$ CD11b$^+$cells, and based on the expression of Ly6C and CD64 within CD11b$^+$ cells, monocytes/macrophages are identified. Expression of CD207 and CD11b was assessed among MHCII^{high} CD11c$^+$ DCs, leading to the identification of CD11b$^+$DDC (CD207$^-$CD11b$^+$), Lang$^+$DDC (CD207$^+$CD11b$^-$), Lang-CD11b$^-$DDCs (CD207$^-$CD11b$^-$) and LCs (CD207$^+$CD11b$^+$). **B)** Bar graph comparing percentage of infiltrating cells detected in ear skin 24 h following application of blank MNs (b-MNs) or MNs laden with b-NPs (b-NPs) or from non-vaccinated mice (control) are shown, as assessed by flow cytometry.

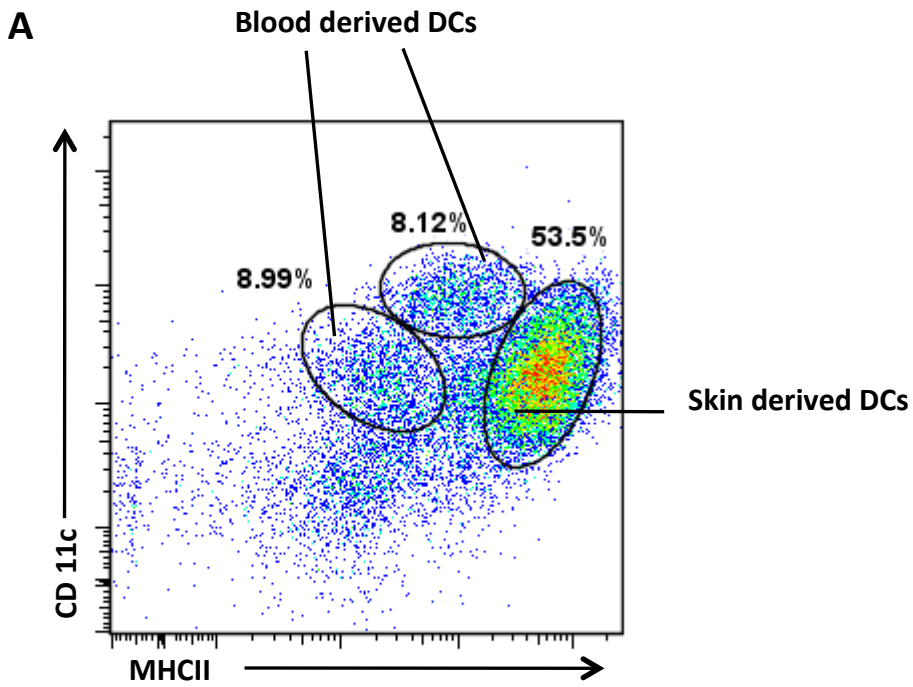

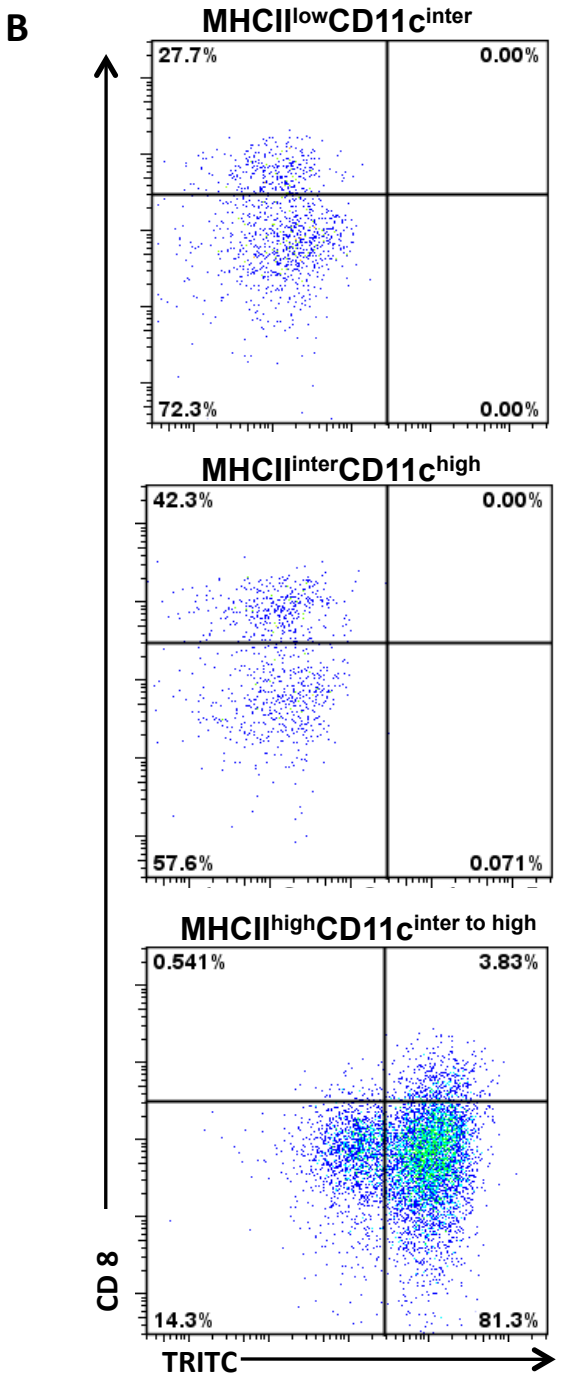

Supplementary Figure 3: Nanoparticles delivered by microneedle application are not taken up by blood derived DC subsets A) Flow cytometry dot plot analysis for the expression of CD11c *versus* MHCII among large cells isolated from the auricular LNs 24 h post MNs mediated TRITC-NPs delivery. As indicated, three populations of DCs can be distinguished in the skin draining LNs, as previously described[48]: skin derived – $MHCII^{high}CD11c^{inter\ to\ high}$ and two blood derived DC subsets – $MHCII^{inter}CD11c^{high}$ and $MHCII^{low}CD11c^{inter}$. **B)** Corresponding DC subsets were separately analyzed for the expression of TRITC and CD8α. All the blood-derived DCs are found to be TRITC negative. Results are representative of two independent experiments.

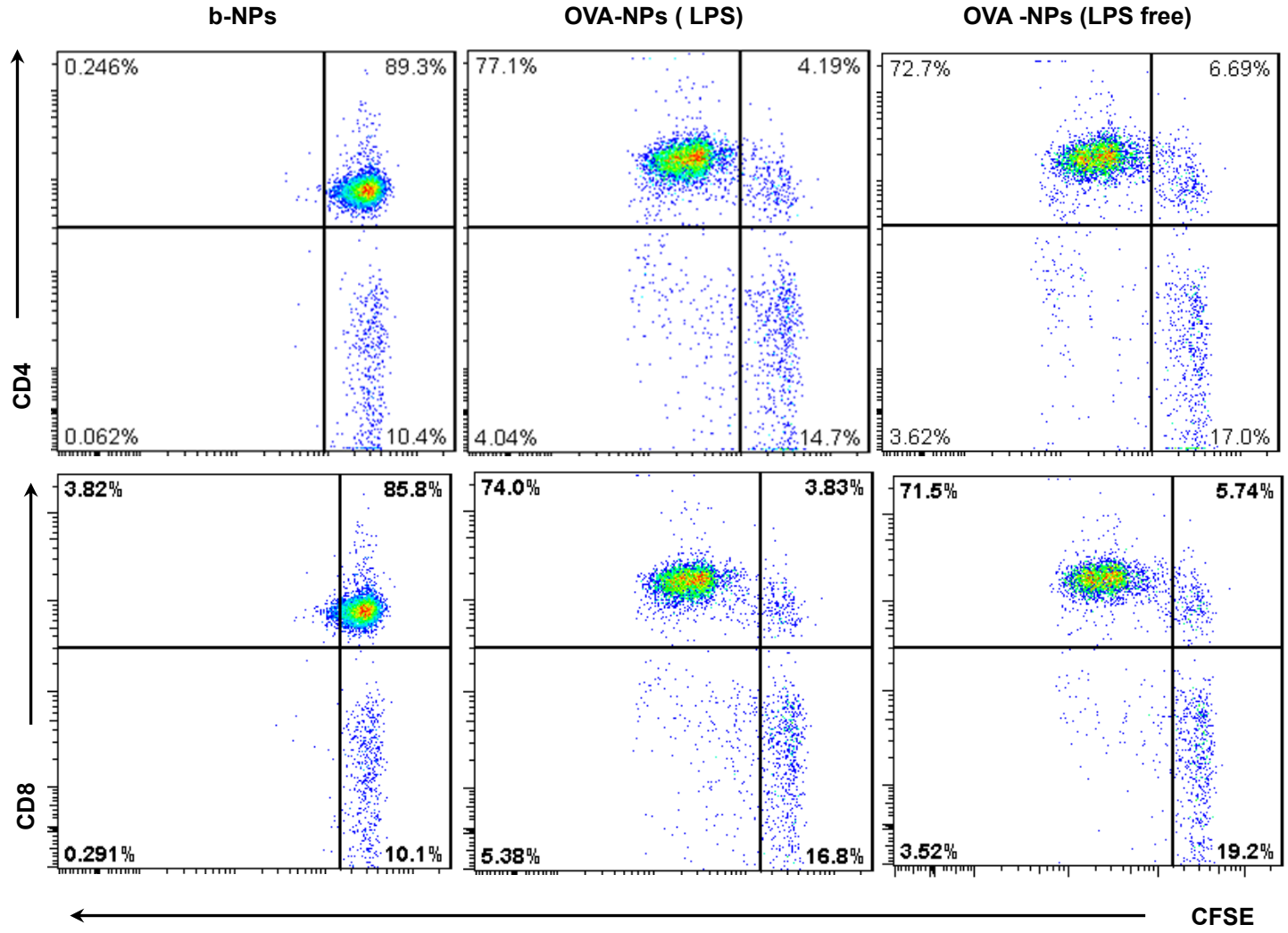

Supplementary Figure 4: OVA derived LPS contamination does not significantly enhance T cell proliferation by skin derived DCs following microneedle immunization. Congenic CD45.1$^+$ mice were injected *i.v.* with CFSE-labeled OVA-specific CD4$^+$ or CD8$^+$ T cells (CD45.2$^+$). The following day, MNs laden with b-NPs, OVA-NPs or LPS-free OVA-NPs were applied to mice ears. Proliferation of OT-I and OT-II cells isolated from auricular LNs was examined 3 days post immunization by flow cytometry. Dot-plots represent CFSE dilutions of CD4$^+$CD45.2$^+$ (*upper panels*) or CD8$^+$CD45.2$^+$ cells (*lower panels*).

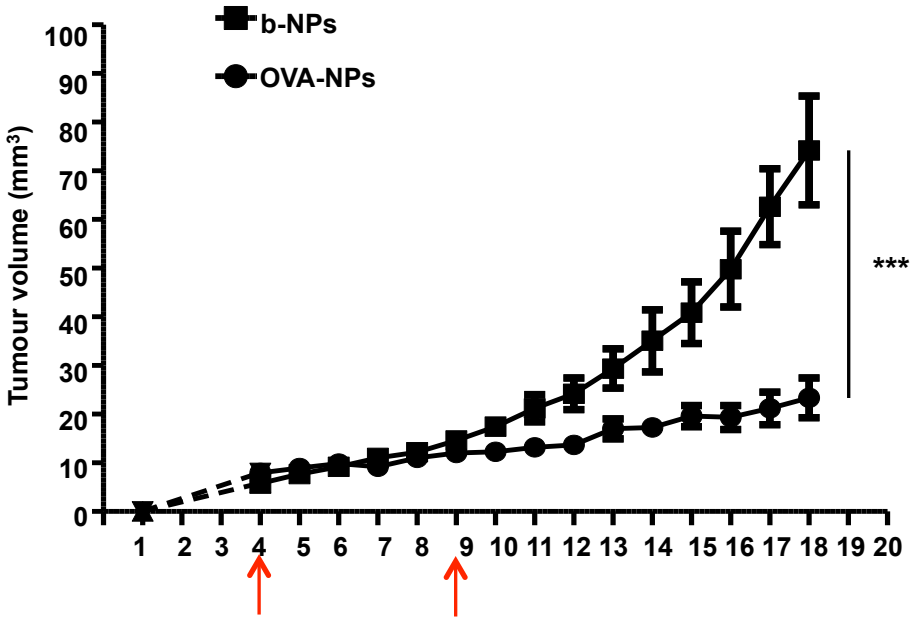

Supplementary Figure 5: Microneedle vaccination of OVA-nanoparticles induces therapeutic anti-tumour responses. Mice were injected with 10^5 B16.OVA melanoma cells, and at days 4 and 9 days (denoted by arrows), mice were immunized with b-NPs or OVA-NPs. Measured tumour volumes in mice treated with b-NPs or OVA-NPs *via* MNs over 18 days post challenge are shown.